Journal of Experimental Nanoscience
Publication details, including instructions for authors and subscription information:
http://www.informaworld.com/smpp/title~content=t716100757

Fabrication of patterned surfaces by photolithographic exposure of DNA hairpins carrying a novel photolabile group

B. Manning[ab]; S. J. Leigh[c]; R. Ramos[a]; J. A. Preece[c]; R. Eritja[a]
[a] Institute for Research in Biomedicine, IQAC-CSIC, CIBER-BBN, Barcelona, Spain [b] School of Chemistry and Chemical Biology, University College Dublin, Ireland [c] School of Chemistry, The University of Birmingham, UK

Online publication date: 08 February 2010

To cite this Article Manning, B. , Leigh, S. J. , Ramos, R. , Preece, J. A. and Eritja, R.(2010) 'Fabrication of patterned surfaces by photolithographic exposure of DNA hairpins carrying a novel photolabile group', Journal of Experimental Nanoscience, 5: 1, 26 — 39
To link to this Article: DOI: 10.1080/17458080903242314
URL: http://dx.doi.org/10.1080/17458080903242314

Journal of Experimental Nanoscience
Vol. 5, No. 1, February 2010, 26–39

Taylor & Francis
Taylor & Francis Group

Fabrication of patterned surfaces by photolithographic exposure of DNA hairpins carrying a novel photolabile group

B. Manning[ab], S.J. Leigh[c], R. Ramos[a], J.A. Preece[c] and R. Eritja[a]*

[a]*Institute for Research in Biomedicine, IQAC-CSIC, CIBER-BBN, Barcelona, Spain;* [b]*School of Chemistry and Chemical Biology, University College Dublin, Ireland;* [c]*School of Chemistry, The University of Birmingham, UK*

(*Received 14 May 2009; final version received 7 August 2009*)

This article demonstrates a method for the fabrication of patterned surfaces using hairpin oligonucleotides carrying a novel photolabile group at the apex of the loop. Photolysis of surfaces carrying photolabile hairpin oligonucleotides results in the formation of areas carrying single-stranded DNA sequences that direct the deposition of the complementary sequence at the photolysed sites. The non-photolysed areas carrying the intact hairpin do not bind to complementary sequences due to the presence of the more stable intramolecular hairpin duplex. The photolithographic process was performed on silicon wafers and followed by atomic force microscopy and epi-fluorescent microscopy. The method described offers an attractive option for the fabrication of biologically interfaced patterned surfaces with specific recognition properties with potential uses in electronics and as biosensors.

Keywords: oligonucleotides; photolysis; AFM; SAM; DNA

1. Introduction

There is a growing interest in the development of efficient methods to self-organise nanoscale components, such as nanoparticles (NPs), nanotubes and biomolecules onto surfaces to fabricate nanostructured systems for electronic or biological or sensing applications [1–4]. Hybrid top-down/bottom-up processes, which combine the precision of lithographic techniques and the parallelism of self-assembly have been actively pursued in order to create patterns on silicon surfaces functionalised with self-assembled monolayers (SAMs) [5–7]. However, the ability to organise biomolecules, such as DNA on surfaces, such as glass [8,9] and gold [10–12] is an area of increased interest.

*Corresponding author. Email: recgma@cid.csic.es

ISSN 1745–8080 print/ISSN 1745–8099 online

DOI: 10.1080/17458080903242314
http://www.informaworld.com

Recent advances in the development of techniques to integrate semiconductor technology with biomolecules have allowed the possibility of utilising the key specific recognition properties of biomolecules to assemble functional devices based on DNA to semiconductor surfaces [13]. The highly specific recognition of complementary strands of oligonucleotides is an ideal way of carrying out highly controlled, precise, species specific self-assembly, where only a specific component carrying the complementary sequence to the surface bound sequence will assemble to that location [14–16].

Methods used previously to pattern surfaces with oligonucleotides have included pre-patterning of the underlying silicon layer by micron-scale UV light exposure of hydrogen-terminated silicon (100) coated with alkenes functionalised with *N*-hydroxysuccinimide ester groups. The resultant *N*-hydroxysuccinimide ester surfaces act as a template for the subsequent covalent attachment of DNA oligonucleotides [17]. A similar effect can be achieved by pre-patterning SAMs on silicon surfaces by electron beam lithography [18]. Other methodologies have utilised soft lithographic techniques, such as contact printing to pattern DNA on surfaces [19]. By introducing the method for patterning of the oligonucleotides surfaces into the DNA oligonucleotide themselves, by way of a photolabile group, a more robust surface patterning technique can be achieved with the possibility for multiple exposure and hybridisation steps once the oligonucleotides are *in situ*, as opposed to a single patterning step before the attachment of the oligonucleotides.

To template the deposition of oligonucleotide sequences onto surfaces to create functional structures, an appropriate surface patterning technique is required, which allows for robust coupling of the oligonucleotide sequences to the surface. One method to create these patterns is by exposure of thiol-stabilised gold NPs supported on silicon wafers to UV light leading to oxidation of the thiol and coagulation of the NPs [20], or photo-crosslinking of C60 derivatives [21], forming dense structures that are resistant to removal by organic solvents. Methods exist to further derivatise gold surfaces, such as those formed, with oligonucleotide sequences [11,22,23]. Alternatively it is possible to modify a specific region of a surface introducing chemical functionality to direct the adsorption of particulate species. As an example, SAMs carrying 4-nitrophenoxy headgroups can be converted to 4-aminophenoxy groups by electron-beam and X-ray irradiation [24]. Selective deposition of citrate-passivated gold NPs to the chemically patterned surfaces can subsequently be achieved due to the affinity of negatively charged gold NPs to protonated amino groups at the surface. The ability to deposit further particulate species to chemically patterned substrates is a robust method for nanostructuring surfaces, as the only change to the surface upon patterning is chemical and not physical.

In an effort to further develop the technique of precision chemical engineering [1], this article describes the attachment of hairpin oligonucleotides to amino functionalised surfaces. Photolithography of the substrates results in the cleavage of the *o*-nitrobenzyl photolabile group at the apex of the hairpin. Subsequent washings lead to the formation of areas with a single-stranded oligonucleotide on the surface. It is then possible to site selectively hybridised complementary oligonucleotide sequences carrying fluorescent molecules or NPs (Scheme 1). In this way the selective deposition of fluorescent molecules or NPs at the photolysed sites can be achieved, allowing further control of the assembly of nanobuilding blocks to surfaces.

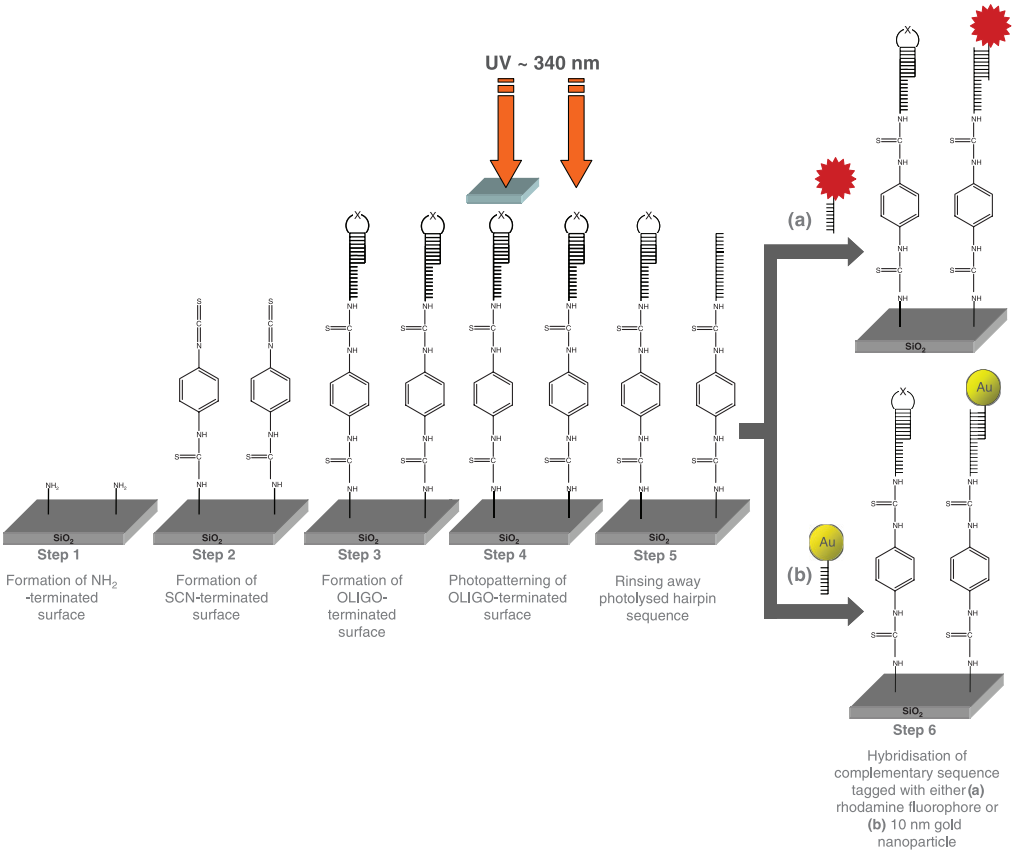

Scheme 1. Scheme of the silicon surface preparation process, photolysis and subsequent hybridisation of either rhodamine or gold NPs labelled complementary sequence as the basis for photopatterning.

2. Experimental section

2.1. *Materials*

Silicon wafers (Si/SiO_2) were purchased from Virginia Semiconductors Inc and were of the type: (a) ⟨111⟩ orientation, (b) resistance of 1–10 $\Omega\,cm^{-1}$, (c) 100 nm (+5%) thick oxide layer on both sides and (d) polished on one side. All commercially available chemicals and solvents were purchased from Fisher Scientific and Sigma Aldrich and used as supplied. Ultra high purity (UHP) H_2O was purified using a UHP filtration system and used with a resistivity of $>18\,M\,\Omega\,cm^{-1}$.

2.2. *Oligonucleotide synthesis*

Oligonucleotide sequences A: 5′-CTCAATGACTCGTT-X-TTCGAGTCATTGAGT CATTTTT-hexyl-NH_2-3′ (X = photolabile linker) and the partially complementary sequence, B: 5′-TGACTCAATGACTCG-propyl-SH-3′ were prepared using the solid-phase methodology as described previously [25]. The photolabile phosphoramidite

(PC spacer-CE phosphoramidite, Link Technologies) was used for the introduction of the photolabile functionality [25]. For the introduction of an amino group at the 3′-end, the 3′-amino-modifier C7 controlled pore glass (CPG) (Glen Research) was used. For the introduction of the thiol group at the 3′-end, the 3′-thiol-modifier CPG (Glen Research) was used. The syntheses were performed on an Applied Biosystems Model 3400 DNA synthesiser using 0.2 and 1 μmol scales. After the assembly of sequences, ammonia deprotection was performed overnight at 55°C. Oligonucleotide carrying the thiol group was deprotected with concentrated ammonia containing 0.05 M 1,4-dithiothreitol (DTT) (16 h, 55°C) and desalted with Sephadex G-25 (NAP-10) prior use. Oligonucleotides were purified by reverse-phase high performance liquid chromatography (HPLC) [25].

The oligonucleotide sequence B carrying 10 nm gold NPs was obtained by reaction of the thiol-oligonucleotide with citrate-stabilised 10 nm gold NPs. The complementary oligonucleotide and 10 nm particles were conjugated using a similar protocol to that first described by Mirkin and Letsinger [26].

The oligonucleotide sequence B carrying rhodamine was obtained by reaction of the 3′-thiol-oligonucleotide with tetramethylrhodamine 5-maleimide (Fluka). The deprotected thiol-oligonucleotide (0.5 ml) was added to a large excess of maleimido-rhodamine (1 mg) and the reaction allowed continuing for 4 h at room temperature. After which the solution was concentrated to dryness and then redissolved in 0.5 mL water. The solution was then purified in a NAP-5 (Sephadex G-25) column and the conjugated rhodamine-complementary oligonucletide was separated from the excess maleimido rhodamine. The desired rhodamine-oligonucleotide was further purified by HPLC [25].

2.3. *Equipment preparation*

Glassware was immersed in piranha solution (70% H_2SO_4, 30% H_2O_2), rinsed and then sonicated in UHP H_2O (resistivity 18 M Ω cm^{-1}) followed by drying in an oven at 127°C for 30 min. Finally the glassware was rinsed and sonicated in ethanol for 30 min before being dried in the oven at 127°C for 24 h prior to use. Clean plastic equipment was rinsed with UHP H_2O for 30 min followed by rinsing with ethanol and a final sonication in ethanol for 30 min.

2.4. *Silicon substrate cleaning*

A silicon wafer was cut into squares of 1 cm^2. They were rinsed with ethanol to clear the surface of any dust produced by the cutting process. The 1 cm^2 squares were then immersed in piranha solution at 90–100°C for 60 min. Once cooled, the piranha solution was rinsed off the substrate with UHP H_2O and each one was sonicated in RCA solution (UHP H_2O; 30% H_2O_2; NH_4OH in a ratio 5 : 1 : 1) for 60 min. Sonication in RCA at this stage functionalises the surface with hydroxyl groups to allow monolayer formation. Repeated rinsing of the substrate in UHP H_2O finishes the cleaning procedure. The substrates were stored in UHP H_2O and used within 2 days to minimise loss of surface hydroxyl groups.

2.5. *Preparation of aminopropylsilane functionalised SAMs*

The cleaned silica substrates were transferred from UHP H_2O into anhydrous ethanol by stepwise exchange from H_2O to ethanol with mixtures in the ratio 3 : 1, 2 : 2, 1 : 3, pure ethanol and finally anhydrous ethanol. The wafers were then immersed into a 0.5 mM solution of (3-aminopropyl)-trimethoxysilane (APTMS) in anhydrous ethanol (5 mL) under a N_2 atmosphere and sonicated at room temperature for 1 h. The substrates were rinsed for 20 s each with ethanol and chloroform, followed by sonication of the wafers twice in fresh ethanol and a final rinsing with ethanol and chloroform. Each sample was then dried under a stream of nitrogen and cured at 120°C for 30 min under vacuum to promote crosslinking of the SAMs

2.6. *Coupling of the photolabile hairpin oligonucleotide to APTMS SAM using p-phenylene diisothiocyanate*

APTMS SAMs were treated with a 0.2% solution of phenylene diisothiocyanate (PDITC) in 10% pyridine/*N*,*N*-dimethylformamide (DMF). After incubation, samples were washed with methanol and acetone and stored in a vacuum dessicator.

A solution carrying 0.68 optical density (OD) units at 260 nm of the photolabile hairpin NH_2 (sequence A) in sodium borate buffer (pH 8.0) was prepared and drop cast onto substrates and incubated at 37° for 2 h. Samples were then washed with 1% NH_4OH, copious amounts of UHP H_2O and methanol. Samples were then dried under a thin stream of N_2 and stored in vacuum desiccator.

2.7. *Photolysis of silica substrates functionalised with the hairpin oligonucleotide*

Silica substrates functionalised with hairpin oligonucleotides were photolysed using a Mercury lamp (Black Eye lamp, 340 nm) for 30 min. It was followed by washing with 200 mM sodium hydroxide and water.

2.8. *UV photolithography*

UV photolithography was carried out using a Suss Microtech MJB4 mask aligner; samples of APTMS SAMs functionalised with the hairpin oligonucleotide were irradiated from 5 s to 1 min with a high intensity UV lamp (340 nm). A mask of vinyl acetate was used for the patterning. After irradiation substrates were washed with 0.2 M NaOH, followed by washing with water and drying under Ar. Before hybridisation the substrate was washed with 1 x SSC and dried under argon. To deactivate remaining isothiocyanate groups the substrates were treated with 50 mM 6-amino-1-hexanol and 150 mM *N*,*N*-diisopropyl-ethylamine in DMF for 2 h and subsequently rinsed with DMF, acetone and dried under argon.

2.9. *Surface hybridisation of complementary oligonucleotide*

A sample of 10 μM complementary rhodamine labelled oligonucleotide in hybridisation buffer (6x SSC, 0.1% SDS, water) was prepared. Hybridisation was carried out for 2 h at room temperature, followed by washing with 6 x SSC, 2 x SSC and water.

2.10. *Surface characterisation*

Samples were analysed via dynamic contact angle measurements, ellipsometry, atomic force microscopy (AFM) and epi-fluorescence microscopy.

2.10.1. *Contact angle*

Water contact angle analysis was carried out using the sessile drop method on a home built contact angle apparatus equipped with a charge-coupled device (CCD) camera attached to a PC for image capture. Contact angles are quoted as the average advancing (Av Adv) and receding (Av Rec) angles from images analysed with software from FTÅ for 5 locations on the same substrate.

2.10.2. *Spectroscopic ellipsometry*

Spectroscopic ellipsometry was carried out using a Jobin-Yvon UVISEL spectroscopic ellipsometer with a white light source. The angle of incidence was fixed at 70° and a wavelength range 250–800 nm was used. Ellipsometric thicknesses were estimated from data taken from a fresh surface in 5 locations and modelled against a cauchy oscillator model.

2.10.3. *Atomic force microscopy*

AFM topography analysis was carried out using a multimode Nanoscope IIIA (Digital Instruments, Santa Barbara, CA) in tapping mode using etched silicon probes.

2.10.4. *Epi-fluorescence microscopy*

Epi-fluorescence images were acquired using a Nikon Eclipse e1000, with a G-2A filter equipped with a Roper coolSNAPfx ccd camera. Images were captured at 20x or 40x in air. Image analysis was carried out using imageJ software and average fluorescence intensities were calculated over the whole image.

3. Results and discussion

3.1. *Design of the photolabile hairpin oligonucleotide*

The aim of the work was to prepare and use an oligonucleotide hairpin having a photolabile group in the apex of the hairpin to fabricate patterns on surfaces. In a previous work, we studied the synthesis and photolysis of peptides and oligonucleotides carrying nitrobenzyl groups in the middle of the sequence [25]. When a photolabile group was introduced in the loop of an intramolecular oligodeoxynucleotide hairpin the intramolecular duplex was converted to an intermolecular duplex with a lower thermal stability [25]. These results suggested that it may be possible to use the photolabile DNA hairpins for the fabrication of patterned surfaces.

To this end we synthesised and immobilised these hairpins to silicon surfaces. Light was used to break the photolabile bond at the loop. In this way half of the hairpin was removed, thus generating areas with an oligonucleotide in single-stranded form (Scheme 1). The single-stranded oligonucleotide regions can be selectively addressed by

the complementary strand allowing the immobilisation of new molecules or nanomaterials at specific sites.

The photolabile hairpin oligonucleotide sequence A (5′-CTCAATGACTCGTT-X-TTCGAGTCATTGAGTCATTTTT-hexyl-NH_2-3′, X = photolabile linker) was synthesised as described previously [25]. A covalent interaction of the oligonucleotide with the surface is the preferred method for attachment of such biomolecules to surfaces to ensure that the biomolecules are not desorbed during further fabrication steps [27]. Oligonucleotide A contains an amino group at the 3′ end [28] followed by 5 thymidines allowing for attachment of the oligonucleotide to surfaces formed from amine-terminated SAMs. The oligonucleotide has a self-complementary sequence of 15 base pairs linked by a tetrathymidine loop. In the middle of the loop there is a photolabile 2-nitrobenzyl group. The phosphoramidite shown in Scheme 2 was used for the introduction of the photolabile 2-nitrobenzyl group at point X in the hairpin (Scheme 1). After ammonia deprotection, the resulting oligonucleotide was purified by reverse-phase HPLC.

3.2. *Silicon surface preparation and characterisation*

Cleaned silicon wafers were functionalised with 3-aminopropyltrimethoxysilane (APTMS) as described previously [29], allowing the formation of amino-terminated surfaces. The APTMS SAM (–NH_2, Scheme 1, Step 1) surfaces were then treated with PDITC to form isothiocyanate terminated surfaces (–SCN, Scheme 1, Step 2) [30–32]. These surfaces were then coupled to the –NH_2 terminated photolabile hairpin oligonucleotide A to form the –OLIGO terminated surfaces (Scheme 1, Step 3).

Dynamic contact angle measurements of APTMS SAM surfaces gave average contact angles of $66^\circ + 7^\circ$ (Av Adv) and $42^\circ + 4^\circ$ (Av Rec), which were slightly higher than some literature values for SAMs fully terminated with NH_2 groups [33]. Ellipsometry measurements showed average APTMS thicknesses of $0.88\,\text{nm} \pm 0.1\,\text{nm}$, which is also comparable to the estimated molecule length (0.69 nm, Chem3D Software), (Table 1), therefore excluding the formation of multilayers as a reason for the slightly higher than expected contact angle values. It is believed that the high contact angle values are therefore due to some disorder being present within the SAM structure.

Dynamic contact angle measurements of −SCN terminated surfaces revealed an increase in contact angle upon formation of −SCN terminated surfaces, which is in good agreement with previously seen behaviour (Table 1) [30]. Ellipsometry of the −SCN terminated surfaces revealed a thickness of $1.2\,\text{nm} \pm 0.2\,\text{nm}$, which is comparable to the estimated thickness of the molecule (1.6 nm, Chem3D Software).

Dynamic contact angle measurements of −OLIGO terminated surfaces revealed a decrease in contact angle upon formation of −OLIGO terminated surfaces (Table 1). The contact angle obtained closely resembles that of the APTMS SAM. We can attribute this similar contact angle to the polar nature of the oligonucleotide and hairpin link added to the surface. The thickness obtained from ellipsometry measurements (10.8 nm) is slightly longer than the estimated length of the oligonucleotide. However, this estimated length does not take into account the length of the photolabile group.

X-ray photoelectron spectroscopy of the silicon based substrates in the region for N (1s) showed the presence of 2 peaks for the APTMS functionalised surfaces (Figure 1). The peak at approximately 400 eV is thought to originate from the NH_2 species of the

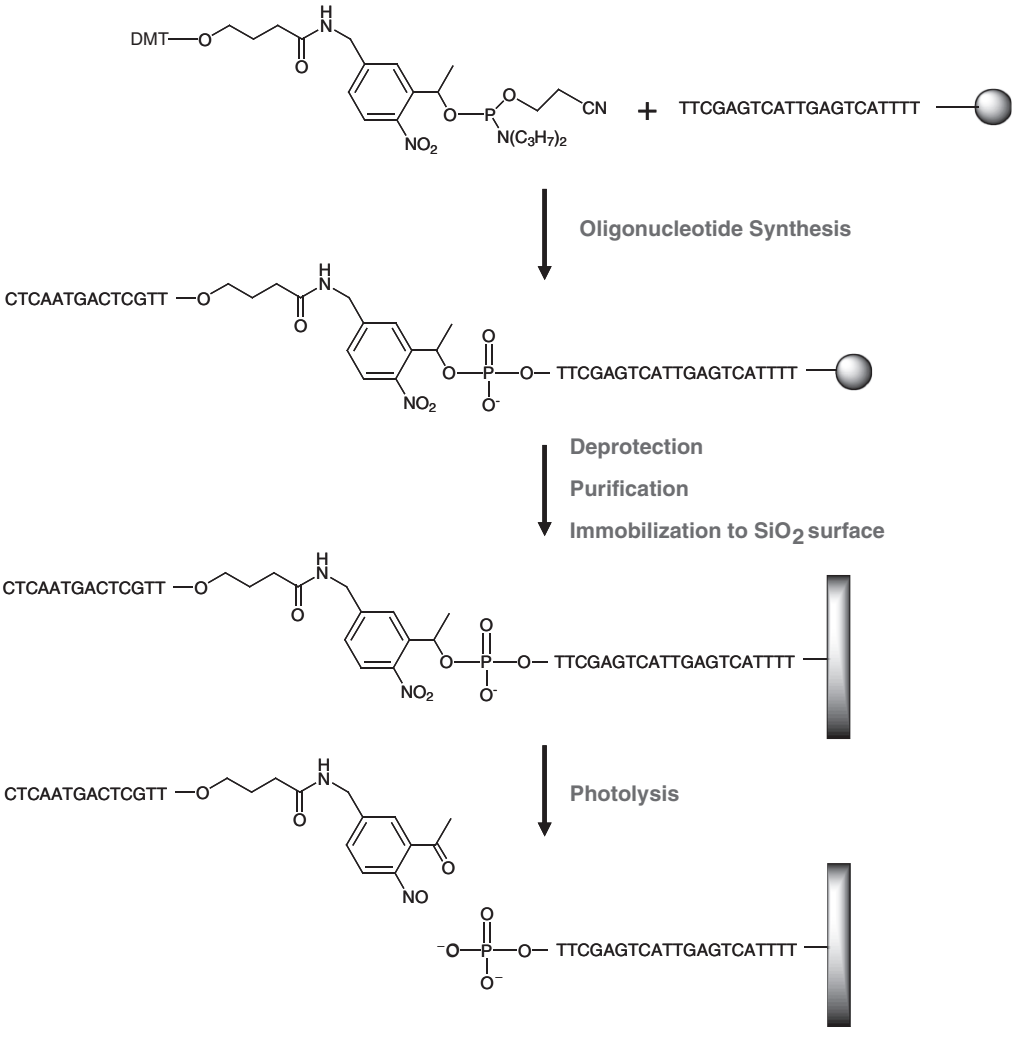

Scheme 2. Synthesis and photocleavage of the hairpin oligonucleotide carrying the 2-nitrobenzyl group (DMT, dimethoxytrityl group).

Table 1. Water contact angles and thickness of functionalised silicon surfaces.

Surface type	Contact angle (Av Adv)	Contact angle (Av Rec)	Ellipsometry thickness (nm)	Expected thickness (nm)
–APTMS	66 ± 7	42 ± 4	0.88 ± 0.1	0.69
–SCN	78 ± 6	51 ± 4	1.2 ± 0.2	1.6
–OLIGO	66 ± 3	39 ± 2	10.8 ± 0.7	8

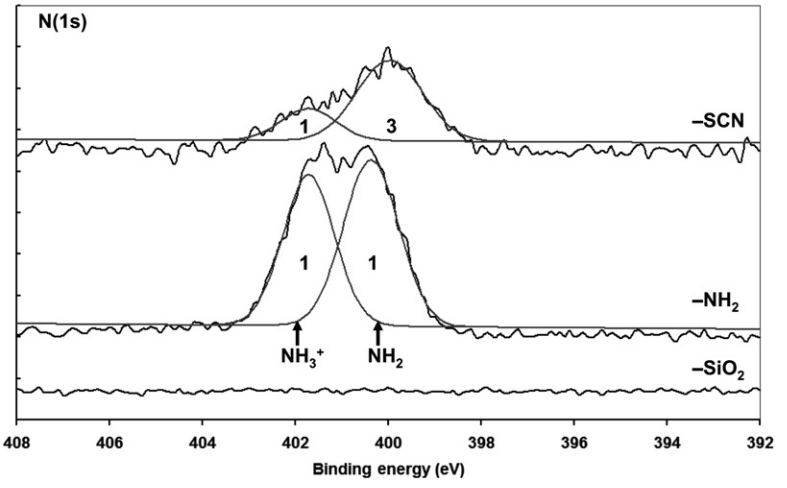

Figure 1. N (1s) X-ray photoelectron spectra of silicon oxide surfaces functionalised with $-NH_2$, and $-SCN$ terminal groups.

APTMS and the second peak at approximately 401.5 eV is thought to originate from the protonated form of the APTMS SAM (NH_3^+) [30]. The two peaks are approximately in a ratio 1 : 1, indicating a 50/50 split in terms of both at the surface. For the $-SCN$ terminated surfaces, the peak at approximately 400 eV is seen to shift and slightly broaden, agreeing with the addition of more nitrogen species ((R(NH)R and C=N–R). The two N1s peaks then exist in a ratio of 3 : 1, indicating that addition of the PDITC species may only occur on 50% of the surface N atoms, possibly due to disorder in the SAM and steric interactions of the PDITC molecule. This observation would also agree with the contact angle values for the NH_2 SAMs showing a slightly disordered SAM. It is believed however that such spacing of the PDITC moieties may be advantageous, as there will be a suitable spacing achieved for the oligonucleotide grafting. Examination of the addition of the oligonucleotide to the silicon surfaces was inconclusive due to broadening of the nitrogen peak, especially in the region between the NH_2 and NH_3^+ regions, consistent with the addition of multiple nitrogen species and especially (N–(C=O)–N) from the high levels of thymine present in the oligonucleotide [30].

AFM images of the $-SCN$ and $-OLIGO$ functionalised surfaces are shown in Figure 2 (Steps 2 and 3). Upon attachment of the hairpin oligonucleotide to the surface, there is an increase in the surface Root mean square (Rms) roughness from 0.214 to 0.659 nm due to the presence and orientation of the hairpin oligonucleotide. The low value for the roughness of the APTMS layer is also further evidence of some disorder of the APTMS chains giving rise to an apparent smoothing of the underlying surface.

3.3. *Surface photolysis*

Upon photolysis of oligonucleotide functionalised surfaces, AFM images show a decrease in Rms roughness from 0.659 to 0.384 nm (Figure 2, Step 5). This decrease may be attributed to the formation of a single stranded oligonucleotide on the surface, which has

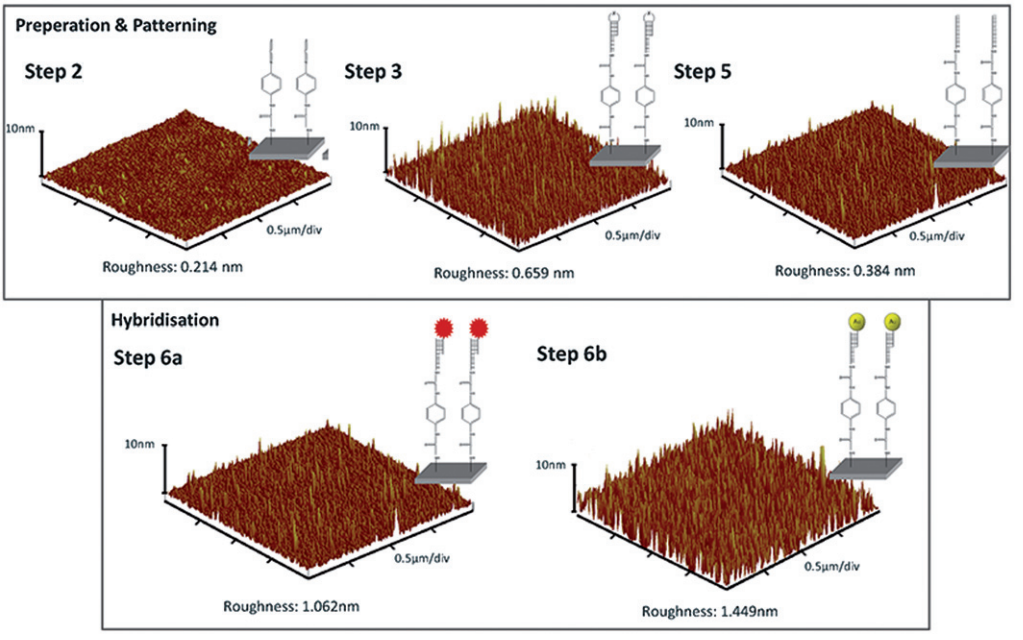

Figure 2. AFM images of SiO_2 surface functionalised with isothiocianate groups (Step 2), the same surface after reaction with 3′-amino hairpin oligonucleotide sequence (Step 3), the same surface after photolysis and rinsing (Step 5), after hybridisation with complementary sequence labelled with rhodamine (Step 6a) or after hybridisation with complementary sequence labelled with 10 nm gold NPs (Step 6b).

a shorter persistence length caused by self-coiling of the single stranded oligonucleotide. Ellipsometry analysis showed a drop in oligonucleotide layer thickness to 1.3 ± 0.6 nm after photolysis and rinsing, which is consistent with photolysis of the photolabile hairpin group and collapse of the single stranded oligonucleotide.

Hybridisation of the photolysed surfaces with complementary oligonucleotide labelled with rhodamine (Figure 2, Step 6a) or gold NPs (Figure 2, Step 6b) produced an increase in roughness seen by AFM (Rms 1.062 and 1.449 nm, respectively). The roughness of the NP surface appears greater than the rhodamine labelled surface due to the size difference between the 5 nm gold NPs and the molecular size rhodamine label. The rhodamine labelled surface appears of a similar roughness to the original non-photolysed sample by AFM, due to the return of a double stranded oligonucleotide on the surface and its associated increase in persistence length. Epifluorescence images of the surfaces showed a strong fluorescent signal from the sample hybridised with the complementary rhodamine oligonucleotide (Figure 3). After denaturing using NaOH the fluorescence decreases dramatically, indicating nearly complete removal of the rhodamine labelled oligonucleotide from the surface and the ability to disassemble the hybridised structures after they have been formed. The surfaces treated with NaOH were hybridised a second time with the complementary rhodamine oligonucleotide and the surfaces showed again a strong fluorescent signal. We have performed three cycles of hybridisation and denaturation without apparent loss of fluorescence indicating the robustness of the immobilisation method and the reversibility of the denaturation process.

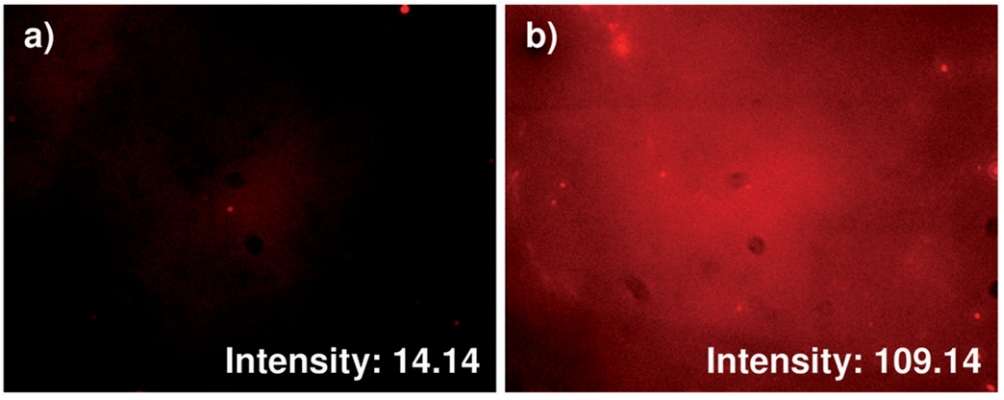

Figure 3. Assesment of intramolecular *versus* intermolecular duplex formation by photolysis and subsequent hybridisation. Two silicon surfaces were functionalised with hairpin oligonucleotide A. One surface was photolysed with UV light (right) while the other was not photolysed (left). Hybridisation with the complementary oligonucleotide labelled with rhodamine showed a more intense fluorescence at the photolysed surface (right). Inset are the average fluorescence intensities of the unphotolysed/photolysed surfaces in arbitrary units (a.u.).

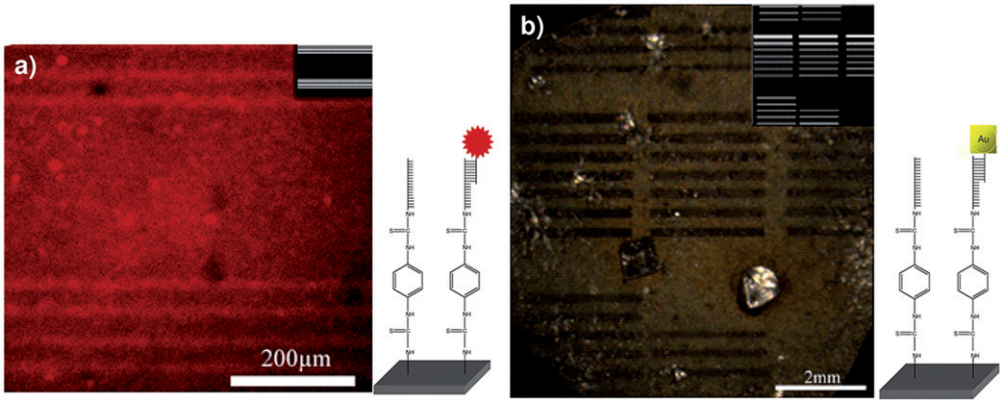

Figure 4. (a) Fluorescent image after photo-patterning and hybridisation with complementary sequence labelled with rhodamine (Step 6a) (inset: image of the calibration mask used in the photolysis) is shown. (b) Optical microscopy image after photo-patterning and hybridisation with complementary sequence labelled with 10 nm gold NPs (Step 6b). The visible lines are areas that were masked during photolysis and hence have no NPs attached. Photography obtained with a stereomicroscope with lateral illumination (inset: image of the calibration mask used in the photolysis).

3.4. *Photopatterning*

Patterning experiments of silicon oxide surfaces carrying hairpin oligonucleotides by UV photolithography were performed. Samples of silicon oxide surfaces functionalised with the hairpin oligonucleotide were irradiated from 5 s to 1 min with a high intensity lamp through a calibration mask of vinyl acetate with lines ranging from 4 to 170 µm.

After irradiation, substrates were washed and hybridised with complementary rhodamine labelled oligonucleotide or gold NPs. Best results were obtained with 1 min irradiation time. Figure 4a shows a fluorescent strip observed by epifluorescence. The pattern of 4 lines from the mask was easily observed, although there is some fluorescence background due to non-specific adsorption. A similar experiment was performed using the complementary oligonucleotide linked to 5 nm gold NPs. The pattern of the mask formed by gold NPs on the surface could be easily observed with lateral light (Figure 4b). Although most of the NPs were in the photolysed areas, some NPs were observed by AFM in the non-photolysed areas due to non-specific adsorption. Further work is needed to reduce non-specific adsorption in non-photolysed areas by using blocking agents such as polyethyleneglycol or albumine or by increasing the length of the oligonucleotide.

4. Conclusions

In summary, we have shown that a hairpin oligonucleotide carrying a photolabile group at the loop provides a simple route for the formation of micrometre-scale patterns on silicon wafers. The process allows for patterning of DNA oligonucleotides *in situ*, negating the need for a pre-patterning step on the surface if required. The ability to attach photolabile oligonucleotides to amino-terminated semiconductor surfaces allows existing techniques for chemically patterning semiconductor surfaces to be further exploited in the formation of nanostructured surfaces comprised of SAMs and DNA oligonucleotides. Exposure of surfaces functionalised with the hairpin to UV light causes the formation of areas functionalised with single stranded oligonucleotides that direct specific deposition of fluorescent compounds or NPs using the complementary oligonucleotide sequence. Due to the specific self-assembling properties of DNA and the existing methods for the synthesis of oligonucleotides it is expected that the set of methods described here may find a wide use for the fabrication of functional nanostructured systems for electronic, biological and sensing applications.

Acknowledgements

This study was supported by the European communities (NANO-3D NMP4-CT2005-014006, DYNAMO NEST-2004-ADV-028669), the Spanish Ministry of Education (NAN2004-09415-C05-03 and BFU2007-63287), the Generalitat de Catalunya (2005/SGR/00693) and the Instituto de Salud Carlos III (CIBER-BNN, CB06_01_0019). We thank the IBEC, PCB and Scientific Services of University of Barcelona to facilitate the use of their instrumentation.

References

[1] P.M. Mendes and J.A. Preece, *Precission chemical engineering: Integrating nanolithography and nanoassembly*, Curr. Opin. Coll. Interf. Sci. 9 (2004), pp. 236–248.
[2] P. Ball, *Chemistry meets computing*, Nature 406 (2000), pp. 118–120.
[3] G. Demirel, M.O. Çaglayan, B. Garipcan, and E. Piskin, *A novel DNA biosensor based on ellipsometry*, Surf. Sci. 602 (2008), pp. 952–959.
[4] P. Kavanagh and D. Leech, *Redox polymer and probe DNA tethered to gold electrodes for enzyme-amplified amperometric detection of DNA hybridization*, Anal. Chem. 78 (2006), pp. 2710–2716.

[5] S. Diegoli, C.A.E. Hamlett, S. Leigh, P.M. Mendes, and J.A. Preece, *Engineering nanostructures at surfaces using nanolithography*, Proc. IMechE G: J. Aerospace Eng. 221 (2007), pp. 589–629.
[6] A. del Campo, D. Boos, H.W. Spiess, and U. Jonas, *Surface modification with orthogonal photosensitive silanes for sequential chemical lithography and site-selective particle deposition*, Angew. Chem. Int. Ed. 44 (2005), pp. 4707–4712.
[7] U. Jonas, A. del Campo, C. Krüger, G. Glasser, and D. Boos, *Colloidal assemblies on patterned silane layers*, Proc. Natl Acad. Sci. USA 99 (2002), pp. 5034–5039.
[8] B. Joos, H. Kuster, and R. Cone, *Covalent attachment of hybridisable oligonucleotides to glass supports*, Anal. Biochem. 247 (1997), pp. 96–101.
[9] R. Fernandes, H. Yi, L.Q. Wu, G.W. Rubloff, R. Ghodssi, W.E. Bentley, and G.F. Payne, *Thermo-biolithography: A technique for patterning nucleic acids and proteins*, Langmuir 20 (2004), pp. 906–913.
[10] C. Boozer, S. Chen, and S. Jiang, *Controlling DNA orientation on mixed ssDNA/OEG SAMs*, Langmuir 22 (2006), pp. 4694–4698.
[11] K. Mukumoto, K. Ohtsuka, T. Nojima, and S. Takenaka, *Preparation of carbodiimide-terminated dithiolane self-assembly monolayers as a new DNA-immobilization method*, Anal. Sci. 22 (2006), pp. 349–355.
[12] S. Tombelli, M. Mascini, and A.P.F. Turner, *Improved procedures for immobilization of oligonucleotides on gold-coated piezoelectric quartz crystals*, Biosens. Bioelectron. 17 (2002), pp. 929–936.
[13] J. Berganza, G. Olabaria, R. García, D. Verdoy, A. Rebollo, and S. Arana, *DNA microdevice for electrochemical detection of* Escherichia coli *0157: H7 molecular markers*, Biosens. Bioelectron. 22 (2007), pp. 2132–2137.
[14] Y. Sakao, F. Nakamura, N. Ueno, and M. Hara, *Hybridization of oligonucleotide by using DNA self-assembled monolayer*, Colloids Surf. B 40 (2005), pp. 149–152.
[15] J. Ladd, C. Boozer, Q. Yu, S. Chen, J. Homola, and S. Jiang, *DNA-directed protein immobilization on mixed self-assembled monolayers via a streptavidin bridge*, Langmuir 20 (2004), pp. 8090–8095.
[16] K. Kerman, Y. Morita, Y. Takamura, M. Ozsos, and E. Tamiya, *Modification of* Escherichia coli *single-stranded DNA binding protein with gold nanoparticles for electrochemical detection of DNA hybridization*, Anal. Chim. Acta 510 (2004), pp. 169–174.
[17] H.B. Yin, T. Briwn, R. Greef, S. Mailis, R. Eason, J.S. Wilkinson, and T. Melvin, *Photo-patterning of DNA oligonucleotides on silicon surfaces with micron-scale dimensions*, Proc. SPIE 5461 (2004), pp. 1–8.
[18] G.J. Zhang, T. Tanii, T. Funatsu, and I. Ohdomari, *Patterning of DNA nanostructures on silicon surface by electron beam lithography of self-assembled monolayer*, Chem. Commun. (2004), pp. 786–787.
[19] P. Björk, S. Holmström, and O. Inganäs, *Soft lithographic printing of patterns of streched DNA and DNA/electronic polymer wires by surface-energy modification and transfer*, Small 2 (2006), pp. 1068–1074.
[20] S. Sun, P.M. Mendes, K. Critchley, S. Diegoli, M. Hanwell, S.D. Evans, G.J. Leggett, J.A. Preece, and T.M. Richardson, *Fabrication of gold micro and nanostructures by photolithographic exposure of thiol-stabilized gold nanoparticles*, Nano Lett. 6 (2006), pp. 345–350.
[21] P. Iqbal, S. Sun, M.D. Hanwell, D. Attwood, G.J. Leggett, J.A. Preece, T.H. Richardson, and D.J. Tunnicliffe, *Photochemical fabrication of three-dimensional micro- and nano-structured surfaces from a C60 monoadduct*, J. Mater. Chem. 18 (2008), pp. 2016–2021.
[22] E. Huang, M. Satjapipat, S. Han, and F. Zhou, *Surface structure and coverage of an oligonucleotide probe tethered onto a gold substrate and its hybridization efficiency for a polynucleotide target*, Langmuir 17 (2001), pp. 1215–1224.

[23] M. Satjapipat, R. Sanedrin, and F. Zhou, *Selective desorption of alkanethiols in mixed self-asssembled monolayers for subsequent oligonucleotide attachment and DNA hybridization*, Langmuir 17 (2001), pp. 7637–7644.
[24] P.M. Mendes, S. Jacke, K. Critchley, J. Plaza, Y. Chen, K. Nikitin, R.E. Palmer, J.A. Preece, S.D. Evans, and D. Fitzmaurice, *Gold nanoparticle patterning of silicon wafers using chemical e-beam lithography*, Langmuir 20 (2004), pp. 3766–3768.
[25] R. Ramos, B. Manning, A. Aviñó, R. Gargallo, and R. Eritja, *Photocleavage of peptides and oligodeoxynucleotides carrying 2-nitrobenzyl groups*, Helv. Chim. Acta 92 (2009), pp. 613–622.
[26] C.A. Mirkin, R.L. Letsinger, R.C. Mucic, and J.J. Storhoff, *A DNA-based method for rationally assembling nanoparticles into macroscopic materials*, Nature 382 (1996), pp. 607–609.
[27] M.R. Lockett, M.F. Phillips, J.L. Jarecki, D. Peelen, and L.M. Smith, *A tetrafluorophenyl activated ester self-assembled monolayer for the immobilization of amino-modified oligonucleotides*, Langmuir 24 (2008), pp. 69–75.
[28] P.S. Nelson, M. Kent, and S. Muthini, *Oligonucleotide labelling methods. 3. Direct labeling of oligonucleotides employing a novel, non-nucleosidic, 2-aminobutyl-1,3-propanediol backbone*., Nucleic Acids Res. 20 (1992), pp. 6253–6259.
[29] S. Diegoli, P.M. Mendes, E.R. Baguley, S.J. Leigh, P. Iqbal, Y.R. García Díaz, S. Begum, K. Critchley, G.D. Hammond, S.D. Evans, D. Attwood, I.P. Jones, and J.A. Preece, *pH-Dependent gold nanoparticle self-organization on functionalized Si/SiO_2 surfaces*, J. Exp. Nanosci. 1 (2006), pp. 333–353.
[30] M.R. Vilar, A.M. Botelho do Rego, A.M. Ferraria, Y. Jugnet, C. Nogues, D. Peled, and R. Naaman, *Interaction of self-assembled monolayers of DNA with electrodes: HREELS and XPS studies*, J. Phys. Chem. B 112 (2008), pp. 6957–6964.
[31] M. Manning and G. Redmond, *Formation and characterization of DNA microarrays at silicon nitride substrates*, Langmuir 21 (2005), pp. 395–402.
[32] M. Manning, P. Galvin, and G. Redmond, *A robust procedure for DNA microarray fabrication and screening in the molecular biology laboratory*, Am. Biotech. Lab. 20 (2002), pp. 16–17.
[33] A.B. Sieval, R. Linke, G. Heij, G. Meijer, H. Zuilhof, and E.J.R. Sudhölter, *Amino-terminated organic monolayers on hydrogen-terminated silicon surfaces*, Langmuir 17 (2001), pp. 7554–7559.